

The Activation of Hydrogen by Li Atoms To Form $[(\text{LiH})_2]^*$

Xuefeng Wang and Lester Andrews*

Lithium hydride is an important molecule. First, it is the lightest metal hydride, which makes it an ideal subject for fundamental experimental and theoretical investigations. Second, lithium hydrides are efficient hydrogen-storage materials because of their large hydrogen mass percentage, and LiH and ternary lithium hydrides (such as LiBH_4 , LiAlH_4 , and Li_3AlH_6) have been examined for hydrogen storage.^[1–5] Hence, the reaction of lithium and hydrogen merits more attention. Although most chemical systems that generate or react with H_2 involve transition-metal centers, reversible hydrogen activation has been accomplished recently with a main-group nonmetal compound.^[6] The important mechanisms for activating and reforming H_2 have been given a chemical perspective.^[7] Third, we have formed $[(\text{LiH})_2]$ in the reaction of 2Li and H_2 , and report the first experimental evidence for the LiH dimer. This dimer is of interest as the simplest example of bridged-hydride structures such as those found in $\text{HBe}(\mu\text{-H})_2\text{BeH}$, $\text{HMg}(\mu\text{-H})_2\text{MgH}$, and $\text{H}_2\text{Al}(\mu\text{-H})_2\text{AlH}_2$ ^[8–10] and for comparison with the “inverse hydrogen bond” $\text{Li-H}\cdots\text{Li-H}$.^[11,12] Furthermore, lithium is the closest congener of hydrogen, and the “lithium bond” has been suggested as an analogue of the pervasive hydrogen bond.^[13]

Lithium atoms are very reactive with the more electronegative molecules, and the reaction with Cl_2 gives LiCl , $[(\text{LiCl})_2]$, and the $[\text{Li}^+\text{Cl}_2^-]$ complex.^[14] The reaction with O_2 produces the $[\text{Li}^+\text{O}_2^-]$ superoxide complex in this favorable charge-transfer reaction.^[15] However, the analogous reaction product with H_2 , namely, $[\text{Li}(\text{H}_2)]$, is higher in energy than the reactants,^[16] and thus such a product does not form in this system.

Unlike the much more stable lithium halides, lithium hydride exists in much lower equilibrium yield and partial pressure in high-temperature reactions of the elements.^[17] This lower yield has so far prevented the observation of $[(\text{LiH})_2]$ in the gas phase, although the diatomic molecule LiH has been characterized by several spectroscopic methods.^[17–21] Over the last several years, we have demonstrated that metal-atom reactions with pure hydrogen on condensation at 4 K give a large yield of metal hydrides and employed this method for the first preparation of dialane.^[8–10,22] Although the reaction of Li and H_2 is unfavorable, the reaction of 2Li

and H_2 to form $[(\text{LiH})_2]$ is exothermic, and this spontaneous reaction at low kinetic but high electronic temperature contributes to the yield of $[(\text{LiH})_2]$ in solid hydrogen.

Laser-ablated Li atoms have been codeposited with excess H_2 at 3.2 K for electronic-spectroscopic investigation of doped solids as high-energy-density materials for rocket propellants. These experiments showed that both Li atoms and Li_2 molecules can be trapped in solid hydrogen and suggested that some reaction with H_2 may also occur, but binary Li_xH_y products were not identified from the electronic spectrum.^[23]

The experimental methods for infrared spectroscopic investigation of laser-ablated metal-atom reactions with hydrogen during condensation at 4 K have been described.^[22] Low laser energy (1–3 mJ per pulse) was employed to avoid ablating lithium clusters. A typical infrared spectrum is illustrated for natural Li (92.6% ^7Li , 7.4% ^6Li) and solid hydrogen in Figure 1. After sample deposition, the region

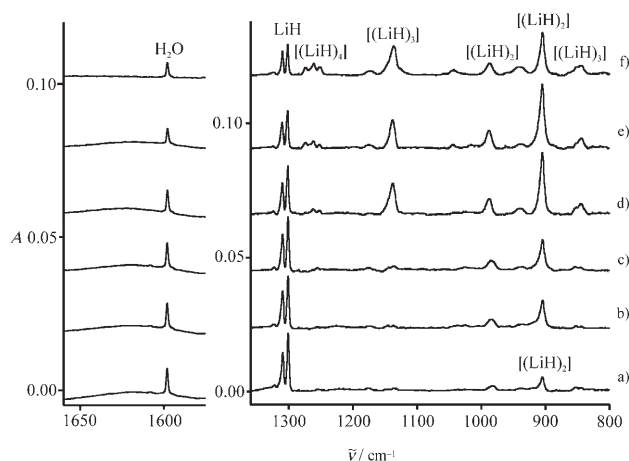


Figure 1. Infrared spectra in the regions 1660–1580 and 1350–800 cm^{-1} for products of the reaction of Li atoms with hydrogen: a) after codeposition of laser-ablated natural-isotopic Li atoms and hydrogen for 30 min at 4 K, b) after annealing to 6.5 K, c) after annealing to 6.8 K, d) after irradiation at $\lambda > 520$ nm, e) after irradiation at $\lambda > 290$ nm, and f) after annealing to 7.3 K.

around 1600 cm^{-1} contained only H_2O at 1598.0 cm^{-1} . A strong, sharp doublet was observed at 1309.9 and 1301.2 cm^{-1} (labeled LiH), and an important new feature was found at 904.7 cm^{-1} (labeled $[(\text{LiH})_2]$; Figure 1a). Annealing the sample first to 6.5 K and then to 6.8 K left the LiH doublet absorbance unchanged, increased the $[(\text{LiH})_2]$ band by 100 %, and produced a very weak new feature at 1138.0 cm^{-1} (labeled $[(\text{LiH})_3]$; Figure 1b,c). Exposure of the sample to radiation from a 175-W mercury-arc lamp ($\lambda > 630\text{ nm}$), which covers the Li absorption,^[23] had no effect on the

[*] Dr. X. Wang, Prof. Dr. L. Andrews
Department of Chemistry
University of Virginia
Charlottesville, VA 22904-4319 (USA)
Fax: (+1) 434-924-3710
E-mail: lsa@virginia.edu
Homepage: <http://www.virginia.edu/chem/people/faculty/andrews/>

[**] This work was supported by NSF Grant CHE03-52487. We gratefully acknowledge the encouragement of Marjorie Hare Andrews.

spectrum, but radiation with $\lambda > 520$ nm, which falls in the long wavelength side of the Li_2 absorption, doubled the band at 904.7 cm^{-1} , increased a clearly associated band at 987.1 cm^{-1} , and markedly increased the feature at 1138.0 cm^{-1} and an associated band at 843.5 cm^{-1} (Figure 1 d). Subsequent irradiation at $\lambda > 290$ nm slightly decreased the above product absorption bands and increased the absorption of a trio of bands at 1274.4 , 1261.8 , and 1252.2 cm^{-1} (labeled $[(\text{LiH})_4]$; Figure 1 e). Annealing to 7.3 K further decreased the above absorption bands, increased the absorption of the trio (Figure 1 f), and removed 10% of the hydrogen sample based on the strong band^[24] near 4150 cm^{-1} . Further sample warming removed all absorption bands. An additional band at 571.2 cm^{-1} (not shown) tracks with the $[(\text{LiH})_2]$ bands. Similar investigations were performed with ^6Li and H_2 and with each metal isotope as well as D_2 , and the expected shifts in product absorption bands were observed.

The ^7LiH fundamental vibration was observed at 1359.1 cm^{-1} in the gas phase,^[18] and the site-split bands at 1309.9 and 1301.2 cm^{-1} are assigned to ^7LiH shifted by interaction with the solid hydrogen environment. The observation of bands for ^6LiH and ^7LiH with relative intensity appropriate for the natural isotopic sample analysis and $^6\text{LiH}/^7\text{LiH}$ frequency ratio (1.0101, 1.0099 for split bands) near that for the harmonic diatomic molecules (1.0104) confirms the assignment to LiH . The observed $^7\text{LiH}/^7\text{LiD}$ frequency ratio (1.3312) is also near the calculated harmonic ratio (1.3326). The matrix shift of 57.9 cm^{-1} (4.3%) for the strong band is due to interaction of H_2 molecules with the positive end of the LiH dipole to give a complex of the form $[(\text{H}_2)_n\text{LiH}]$. Finally, an HD experiment (Figure 2) gave sharp doublets for both ^7LiH and ^7LiD .

The LiH frequency was calculated at the B3LYP level of theory in the harmonic approximation by using a large basis set^[25] to be 1418.9 cm^{-1} and the Li-H bond length to be 1.589 Å . This calculated harmonic frequency is 4.2% too high, but is in the range of agreement expected,^[26] and the calculated bond length is in very good agreement with the gas-phase experimental value (1.5957 Å).^[27]

The bands at 987.1 , 904.7 , and 571.2 cm^{-1} support identification of the rhombic dimer $[(\text{LiH})_2]$ with D_{2h} symmetry (Figure 3) on the basis of the following evidence. The rhombic dimer is the lowest-energy structure,^[11,28] and the frequencies calculated at the B3LYP level of theory in the harmonic approximation with a large basis set^[25] are compared with the observed values in Table 1. The strongest

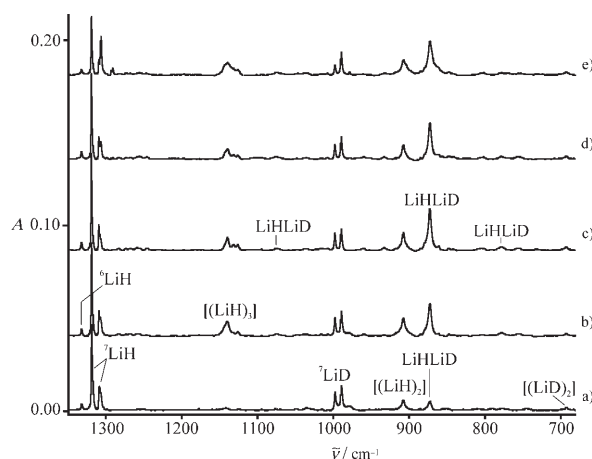


Figure 2. Infrared spectra in the region $1350\text{--}680\text{ cm}^{-1}$ for products of the reaction of Li atoms with HD: a) after codeposition of laser-ablated natural-isotopic Li atoms and HD for 30 min at 4 K , b) after irradiation at $\lambda > 470\text{ nm}$, c) after irradiation at $\lambda > 290\text{ nm}$, d) after annealing to 8 K , and e) after annealing to 9 K .

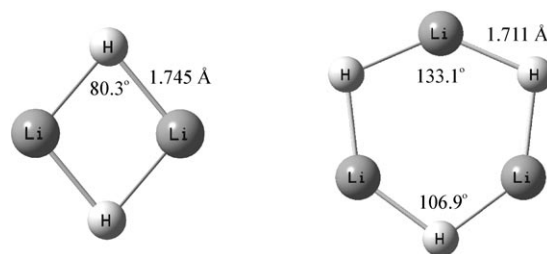


Figure 3. Structures calculated for $[(\text{LiH})_2]$ and $[(\text{LiH})_3]$ with the B3LYP/6-311++G(3df,3pd) method.

infrared-active fundamental vibration is the antisymmetric b_{1u} motion of the H atoms parallel to the Li-Li axis calculated at 970.9 cm^{-1} , and the strongest observed band at 904.7 cm^{-1} is 66.2 cm^{-1} (6.8%) lower. This band shows a $^6\text{LiH}/^7\text{LiH}$ frequency ratio of 1.0095 and a $^7\text{LiH}/^7\text{LiD}$ frequency ratio of 1.3093, which are slightly less than the harmonic ratios calculated for this mode.^[8–10] (The calculated lithium isotopic shift is 1.04%, and the observed shift is 0.95%.) Some of this discrepancy can be attributed to different interactions of H_2 with the Li and H centers of different charges in $[(\text{LiH})_2]$ within the hydrogen matrix. The strong deuterium counter-

Table 1: Observed and calculated frequencies [cm^{-1}] for $[(\text{LiH})_2]$ (1A_g in D_{2h} symmetry).^[a]

mode	obsd	$[(^7\text{LiH})_2]$ calcd	obsd	$[(^6\text{LiH})_2]$ calcd	obsd	$[(^7\text{LiD})_2]$ calcd	obsd	$[(^6\text{LiD})_2]$ calcd	obsd	$^7\text{Li}_2\text{HD}$ calcd
a_g		1174.7(0)		1176.7(0)		841.2(0)		846.0(0)	1076.3	1130.0(386)
b_{2u}	987.1	1079.5(902)	995.7	1090.7(921)	748.0	810.1(508)	761.5	825.0(527)	872.6	933.8(555)
b_{1u}	904.7	970.9(925)	913.3	981.0(944)	691.0	728.6(521)	703.4	742.0(540)	777.6	823.3(318)
b_{3g}		886.7(0)		899.0(0)		677.8(0)		693.8(0)		698.4(168)
b_{3u}	571.2	600.7(699)	574.2	606.9(714)	446	450.8(394)	453	459.0(408)	497.2	531.0(547)
a_g		522.4(0)		563.3(0)		516.1(0)		554.2(0)		519.4(1)

[a] Observed frequencies in solid H_2 , D_2 , or HD. Calculated frequencies at the B3LYP/6-311++G(3df,3pd) level of theory with infrared intensities in kmol^{-1} given in parentheses.

part at 691.0 cm^{-1} exhibits a shoulder at 697.0 cm^{-1} , which is appropriate for the ${}^6\text{LiD}{}^7\text{LiD}$ molecule in natural abundance (note that this frequency is almost half way between the values for pure $[({}^6\text{LiD})_2]$ and $[({}^7\text{LiD})_2]$). The experiment with the pure HD reagent shows the dominant product absorption at 872.6 cm^{-1} upon visible irradiation (Figure 2). ${}^7\text{LiH}{}^7\text{LiD}$ has C_{2v} symmetry, and the modes mix differently to give the strongest absorption calculated for b_1 symmetry at 933.8 cm^{-1} . The strongest product band observed at 872.6 cm^{-1} is 61.2 cm^{-1} (6.6%) lower and follows the above calculated–observed relationship for $[({}^7\text{LiH})_2]$. The next two strongest modes for ${}^7\text{LiH}{}^7\text{LiD}$ are calculated to be 1130.0 and 823.3 cm^{-1} , and the weak bands at 1076.3 and 777.6 cm^{-1} are in accord (observed 5.6 and 5.5% lower). These assignments verify that this product contains two equivalent lithium atoms and two equivalent H atoms, which is a necessary but not sufficient condition for identification of the rhombic $[({}^7\text{LiH})_2]$ molecule.

The two other infrared-active modes for $[(\text{LiH})_2]$ are predicted to be 1079.5 and 600.7 cm^{-1} . The higher-frequency absorption corresponds to the antisymmetric b_{2u} motion of the H atoms perpendicular to the Li–Li axis and is shifted to 987.1 cm^{-1} (8.5% lower), and the lower-frequency absorption is the out-of-plane bending motion, which is shifted to 571.2 cm^{-1} (4.9% lower) by interaction with the H_2 matrix. The upper band exhibits almost the same isotopic frequency ratios (1.0087, 1.3193) as its b_{1u} counterpart, but the lower band exhibits lower 6/7 and H/D isotopic frequency ratios (1.0053, 1.2807), which we believe is due again to different interactions at the Li and H centers. The close relationship between calculated and observed infrared-active fundamental vibrations confirms this first experimental identification of the dimer $[(\text{LiH})_2]$. The harmonic B3LYP frequencies are expected to be slightly higher than the observed values,^[26] and part of this difference is due to anharmonicity and part is due to interaction with the matrix.

We should note that the observed and calculated (B3LYP and MP2 give similar results) infrared intensities for $[(\text{LiH})_2]$ agree only qualitatively. Again, we must remember that the calculation is done in the harmonic approximation for the gaseous ionic molecule, and the observed spectrum is for the molecule trapped in a solid hydrogen matrix. The three IR-active fundamental vibrations for $[(\text{LiH})_2]$ are predicted to have relative intensities of 1/1/0.8 (from highest to lowest wavenumber; Table 1), and the observed absorption bands have relative integrated intensities of 1/2.5/1. The strongest-intensity band at 904.7 cm^{-1} , which involves H motion parallel to the Li–Li axis, is either underestimated by the calculation or more likely enhanced by the matrix environment. One can picture the $[(\text{LiH})_2]$ molecule entrapped in the solid hydrogen lattice, and the b_{2u} mode damped more by the matrix cage than the b_{1u} mode. This point gains credence from the fact that the higher-frequency b_{2u} absorption is broader ($2\times$) than the lower-frequency, sharper b_{1u} band.

The rhombic $[(\text{LiH})_2]$ structure (Figure 3) exhibits a calculated Li...Li distance of 2.250 Å , which is shorter than the computed internuclear distance (B3LYP, 2.702 Å) for the electron-pair bonded Li_2 molecule. In the rhombic structure, however, the Li valence electrons are drawn to the more

electronegative H atoms to form a highly ionic molecule (calculated natural charges of $+0.84$ on Li and -0.84 on H), which leaves little electron density^[11] to bond between the Li centers. The molecular orbitals in Figure 4 show the absence of bonding between the two lithium atoms and the electrostatic nature of the bonding in $[(\text{LiH})_2]$.

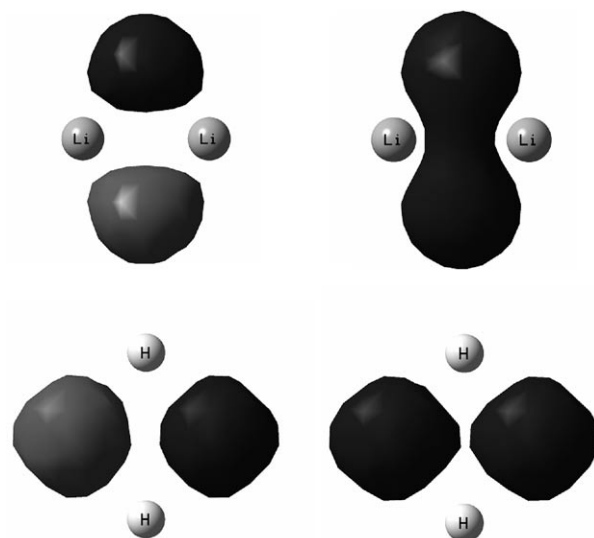


Figure 4. The four occupied molecular orbitals calculated for $[(\text{LiH})_2]$ with the B3LYP/6-311++G(3df,3pd) method. The isoelectronic density level is 0.07 e au^{-3} .

The early electronic-structure calculations on $[(\text{LiH})_2]$ with the simple Hartree–Fock method and minimum basis sets^[11,28] gave longer Li...Li distances (up to 2.39 Å) and a Li–H bond length of 1.81 Å . However, the more rigorous MP2 method and a medium basis set^[11] gave a Li–H bond length of 1.758 Å , which is close to our MP2 result of 1.760 Å and our B3LYP value.

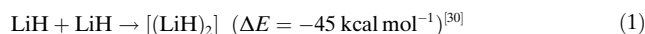
The linear dimer with the inverse hydrogen bond is also an interesting molecule to consider, but this higher-energy species (calculated 22 kcal mol^{-1} , see also reference [28a]) was not observed in this study. Furthermore, the lowest-frequency bending mode is imaginary (also at the MP2 level of theory^[11]), so our calculation suggests that this is a transition state that will bend into the rhombic dimer. The strongest calculated Li–H stretching frequency for the linear dimer is 1675 cm^{-1} and a decrease of 4–6% reasonably predicts this absorption in the region from 1590 to 1630 cm^{-1} , where no product absorption is observed (Figure 1). The more stable rhombus structure is the only lithium hydride dimer observed in this study.

In contrast, the bands at 1138.0 and 843.5 cm^{-1} showed no significant increase upon the annealing that substantially increased the $[(\text{LiH})_2]$ bands, but they increased dramatically upon irradiation at $\lambda > 520\text{ nm}$, which increased the $[(\text{LiH})_2]$ bands twofold. This result invites consideration of a higher cluster, and calculations for $[(\text{LiH})_3]$ converged to the D_{3h} structure given in Figure 3. The highest IR-active frequency calculated for $[(\text{LiH})_3]$ (1229 cm^{-1}) is substantially higher

than that for $[(\text{LiH})_2]$ (1079 cm^{-1}). Also, the calculated $^6\text{LiH}/^7\text{LiH}$ harmonic isotopic frequency ratio (1.0070) for this e mode is less than the ratio (1.0104) for the rhombus structure. The band at 1138.0 cm^{-1} is 91.1 cm^{-1} (8.0%) lower and exhibits a substantially lower $^6\text{LiH}/^7\text{LiH}$ frequency ratio (1.0053) than the modes for the rhombus structure. Furthermore, the computed $^7\text{LiH}/^7\text{LiD}$ ratio (1.3536) is higher than determined for the modes of the dimer, as is the observed ratio (1.3344). Hence, the band at 1138.0 cm^{-1} is due to a coupled Li–H motion in a structure other than the rhombic dimer, and the expected match with the harmonic values computed for $[(\text{LiH})_3]$ substantiates this identification.

The trio of bands at 1274.4 , 1261.8 , and 1252.2 cm^{-1} increased on irradiation at $\lambda > 290\text{ nm}$ and annealing at 7.3 K at the expense of the absorption bands of $[(\text{LiH})_n]$ ($n=1,2,3$) so a still-higher cluster is indicated. Accordingly, calculations were done for $[(\text{LiH})_4]$, and the computed e mode (1376.4 cm^{-1}) of the D_{4h} structure was the strongest absorption. The middle component of the trio is 114.6 cm^{-1} (8.3%) lower and appropriate for this assignment. The isotopic frequency ratios (1.0058, 1.3278) are comparable to those observed for $[(\text{LiH})_3]$.

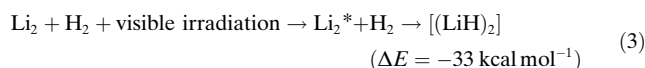
Information on the reaction mechanism is revealed by mixed isotopic reagents. The major product bands on deposition with HD are assigned to LiH and LiD, and $[(\text{LiH})_2]$, LiHLiD, and $[(\text{LiD})_2]$ are observed as well (Figure 2). Visible irradiation increases the band of LiHLiD more than those of the other isotopic species. An investigation with 50/50 H_2/D_2 gave almost equal intensity bands for LiH and LiD, greater intensity of the band for $[(\text{LiH})_2]$ than that of $[(\text{LiD})_2]$, and an intermediate intensity band for LiHLiD. Visible irradiation increased the intensity of the bands for $[(\text{LiH})_2]$ and $[(\text{LiD})_2]$ but not for LiHLiD. These results show that a small amount of $[(\text{LiH})_2]$ is made by dimerization [Eq. (1)] on sample deposition, but that the



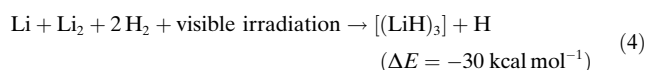
major growth arises from reactions with the H_2 reagent. Annealing prior to irradiation produces $[(\text{LiH})_2]$ in a spontaneous reaction [Eq. (2)] in solid hydrogen at $6\text{--}7\text{ K}$. Since



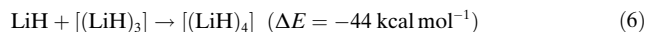
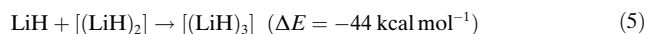
annealing removes lithium atoms^[23] to form Li_2 ,^[29] activation probably arises from the exothermic (24 kcal mol^{-1})^[27] dimerization of two lithium atoms to give excited-state Li_2 , which spontaneously reduces an adjacent dihydrogen molecule to the dilithium dihydride. Even more growth of $[(\text{LiH})_2]$ comes from a photochemical reaction [Eq. (3)] in which Li_2 is excited



directly.^[23] The major formation of trimer also arises from visible irradiation in a reaction such as Equation (4). Finally,



the growth of tetramer on annealing at the expense of $[(\text{LiH})_n]$ ($n=1,2,3$) provides evidence for the exothermic addition reactions Equations (5) and (6).



The novel highly ionic rhombic dimer $[(\text{LiH})_2]$ is the major product of the reaction of lithium atoms in solid H_2 on annealing and on visible irradiation. Thus, two lithium atoms activate dihydrogen in the simplest possible chemical reduction process [Eq. (2)], in this case, at low kinetic but high electronic temperature. Finally, the $[(\text{LiH})_n]$ oligomers investigated herein are expected to decompose at a lower temperature than crystalline LiH, and they have the potential to provide a more useful source of hydrogen gas.

Received: December 22, 2006

Revised: January 22, 2007

Published online: March 2, 2007

Keywords: density functional calculations · dimerization · H–H activation · hydrogen · lithium

- [1] M. S. Dresselhaus, I. L. Thomas, *Nature* **2001**, *414*, 332.
- [2] L. Schlappbach, A. Züttel, *Nature* **2001**, *414*, 353.
- [3] W. Grochala, P. P. Edwards, *Chem. Rev.* **2004**, *104*, 1283.
- [4] V. P. Balema, J. W. Wiench, K. W. Denis, M. Pruski, V. K. Pecharsky, *J. Alloys Compd.* **2001**, *329*, 108.
- [5] V. C. Y. Kong, D. W. Kirk, F. R. Foulkes, J. T. Hinatsa, *Int. J. Hydrogen Energy* **2003**, *28*, 205.
- [6] G. C. Welch, R. R. San Juan, J. D. Masuda, D. W. Stephan, *Science* **2006**, *314*, 1124.
- [7] G. J. Kubas, *Science* **2006**, *314*, 1096.
- [8] Be + H_2 : X. Wang, L. Andrews, *Inorg. Chem.* **2005**, *44*, 610.
- [9] Mg + H_2 : X. Wang, L. Andrews, *J. Phys. Chem. A* **2004**, *108*, 11511.
- [10] Al + H_2 : a) L. Andrews, X. Wang, *Science* **2003**, *299*, 2049; b) X. Wang, L. Andrews, S. Tam, M. E. DeRose, M. Fajardo, *J. Am. Chem. Soc.* **2003**, *125*, 9218.
- [11] I. Rozas, I. Alkorta, J. Elguero, *J. Phys. Chem. A* **1997**, *101*, 4236.
- [12] S. A. C. McDowell, *J. Comput. Chem.* **2003**, *24*, 1201.
- [13] A. B. Sannigrahi, T. Kar, B. G. Niyogi, P. Hobza, P. v. R. Schleyer, *Chem. Rev.* **1990**, *90*, 1061.
- [14] W. F. Howard, Jr., L. Andrews, *Inorg. Chem.* **1975**, *14*, 767.
- [15] L. Andrews, *J. Chem. Phys.* **1969**, *50*, 4288.
- [16] a) P. Hobza, P. v. R. Schleyer, *Chem. Phys. Letts.* **1984**, *105*, 630; b) A. I. Boldyrev, J. Simons, *J. Chem. Phys.* **1993**, *99*, 4628.
- [17] a) T. C. James, W. G. Norris, W. Klemperer, *J. Chem. Phys.* **1960**, *32*, 728; b) L. Wharton, L. P. Gold, W. Klemperer, *J. Chem. Phys.* **1960**, *33*, 1255.
- [18] C. Yamada, E. Hirota, *J. Chem. Phys.* **1988**, *88*, 6702.
- [19] A. G. Maki, W. B. Olson, G. Thompson, *J. Mol. Spectrosc.* **1990**, *144*, 257.
- [20] H. W. Sarkas, J. H. Hendricks, S. T. Arnold, K. H. Bowen, *J. Chem. Phys.* **1994**, *100*, 1884.
- [21] N. Bouloufa, L. Cabaret, P. Luc, R. Vetter, W. T. Luh, *J. Chem. Phys.* **2004**, *121*, 7237.
- [22] L. Andrews, *Chem. Soc. Rev.* **2004**, *33*, 123, and references therein.
- [23] M. E. Fajardo, *J. Chem. Phys.* **1993**, *98*, 110.
- [24] H/ H_2 : L. Andrews, X. Wang, *J. Phys. Chem. A* **2004**, *108*, 3879, and references therein.

- [25] Gaussian98 (Revision A.7), M. J. Frisch, G. W. Trucks, H. B. Schlegel, G. E. Scuseria, M. A. Robb, J. R. Cheeseman, V. G. Zakrzewski, J. A. Montgomery, R. E. Stratmann, J. C. Burant, S. Dapprich, J. M. Millam, A. D. Daniels, K. N. Kudin, M. C. Strain, O. Farkas, J. Tomasi, V. Barone, M. Cossi, R. Cammi, B. Mennucci, C. Pomelli, C. Adamo, S. Clifford, J. Ochterski, G. A. Petersson, P. Y. Ayala, Q. Cui, K. Morokuma, D. K. Malick, A. D. Rabuck, K. Raghavachari, J. B. Foresman, J. Cioslowski, J. V. Ortiz, B. B. Stefanov, G. Liu, A. Liashenko, P. Piskorz, I. Komaromi, R. Gomperts, R. L. Martin, D. J. Fox, T. Keith, M. A. Al-Laham, C. Y. Peng, A. Nanayakkara, C. Gonzalez, M. Challacombe, P. M. W. Gill, B. G. Johnson, W. Chen, M. W. Wong, J. L. Andres, M. Head-Gordon, E. S. Replogle, J. A. Pople, Gaussian, Inc., Pittsburgh, PA, **1998**, and references therein.
- [26] a) A. P. Scott, L. Radom, *J. Phys. Chem.* **1996**, *100*, 16502; b) M. P. Andersson, P. L. Uvdal, *J. Phys. Chem. A* **2005**, *109*, 2937.
- [27] *Constants of Diatomic Molecules*, K. P. Huber, G. Herzberg, Van Nostrand-Reinhold, New York, **1979**.
- [28] a) D. J. Defrees, K. Raghavachari, H. B. Schlegel, J. A. Pople, P. v. R. Schleyer, *J. Phys. Chem.* **1987**, *91*, 1857, and references therein; b) K. S. Rao, S. N. Khanna, P. Jena, *Phys. Rev. B* **1991**, *43*, 1416, and references therein.
- [29] L. Andrews, G. C. Pimentel, *J. Chem. Phys.* **1967**, *47*, 2905.
- [30] Reaction energies calculated by B3LYP/DFT with zero-point-energy correction.
-